ACS OMEGA

http://pubs.acs.org/journal/acsodf

Article

Computational Analysis of Vibrational Spectra of Hydrogen Bonds in sII and sH Gas Hydrates

Qing Guo, Hao-Cheng Wang, Xiao-Yan Liu, Xiao-Qing Yuan, Xiao-Tong Dong, Yi-Ning Li, Yi Yin, and Peng Zhang*

Cite This: *ACS Omega* 2023, 8, 11634−11639

Read Online

ACCESS | Metrics & More | Article Recommendations | Supporting Information

ABSTRACT: The amount of energy in natural gas hydrates is thought to be equivalent to twice that of all other fossil fuels combined. However, economic and safe energy recovery has remained a challenge till now. To develop a novel method of breaking the hydrogen bonds (HBs) surrounding the trapped gas molecules, we investigated the vibrational spectra of the HBs of gas hydrates with structure types II and H. Two models of 576-atom propane−methane sII hydrate and 294-atom neohexane−methane sH hydrate were built. A first-principles density functional theory (DFT) method was employed using the CASTEP package. The simulated spectra were in good agreement with the experimental data. Compared with the partial phonon density of states of guest molecules, we confirmed that the experimental infrared absorption peak in the terahertz region mainly arose from HB vibrations. By removing the components of guest molecules, we found that the theory of two kinds of hydrogen bond vibrational modes applies. The use of a terahertz laser to enable resonance absorption of HBs (at about 6 THz, to be tested) may therefore lead to the rapid melting of clathrate ice and release of guest molecules.

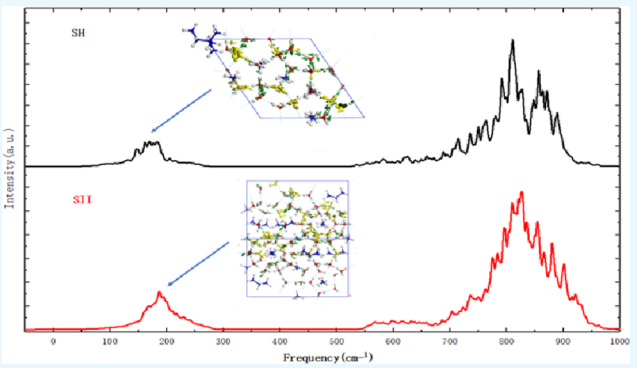

INTRODUCTION

Natural gas hydrates are nonstoichiometric inclusion compounds formed by guest hydrocarbon gas and a host molecule (water) under high pressure and low temperature. Due to their high energy density, each volume of gas hydrate can produce up to 180 volumes of gas. It has been estimated that natural gas hydrates have twice the amount of energy of current fossil fuel reserves.[1] However, the recovery of methane from gas hydrates has not been commercialized due to economic and safety constraints. The dissociation of gas hydrates represents the breaking of intermolecular hydrogen bonds (HBs). Investigating the lattice dynamics of HBs may shed light on new possibilities in this realm.

Due to the different sizes of gas molecules and cage structures, the most common clathrate hydrates occur as one of three crystal structures: cubic structure I (sI), face-centered cubic structure II (sII), and hexagonal structure H (sH). The sI and sII structures were determined in the 1940s by Stackelberg and Muller, and sH was discovered in 1987 by Ripmeester et al.[2−4] Both the sI and sII structures are composed of small 5^{12} (pentagonal dodecahedron) cages. As pentagons cannot fill the whole space, an additional large cage $5^{12}6^2$ ($5^{12}6^4$) is needed for sI (sII) to prevent HB fracture. sH has two additional medium ($4^35^66^3$) cavities and one large cavity ($5^{12}6^8$). Typical sII guest molecules are nitrogen, propane, and isobutane.[1] They form when gas molecules interact with water near gas pipelines or deep ocean areas. sH requires both small (e.g., methane) and large molecules (e.g., 2,2-dimethylbutane, 2-methylbutane) present in crude oils.[5] Following concerns in the oil industry, Falenty et al. evacuated guest molecules from sII hydrate in laboratory experiments and found that an empty clathrate hydrate framework could exist stably and was named ice XVI.[6] Later, Rosso et al. obtained a nonguest sI type ice clathrate, named XVII.[7]

Spectroscopic investigations are currently the most extensively used techniques to obtain structural information and determine the thermodynamic properties of gas hydrates. Schicks et al. reported the coexistence of sI and sII methane hydrate by Raman spectroscopy.[8] Murshed et al. showed that sII methane hydrate could be obtained by adding a second gas, such as ethane.[9] Sum et al. were the first to report the cage occupancy and water number of methane hydrates under different equilibrium conditions.[10] Jin et al. studied the decomposition of methane hydrate via attenuated total reflection infrared (IR) spectroscopy.[11] Many inelastic neutron

Received: February 23, 2023
Accepted: March 3, 2023
Published: March 13, 2023

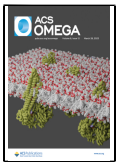

scattering (INS) experiments examined the far-IR regions of gas hydrates.[12−15] Since Tse first studied guest−host coupling using molecular dynamics simulations, many researchers have theoretically studied molecular vibrations.[16−19] Based on a series of investigations of the lattice dynamics of ice phases, we found that the main vibration modes of HB can be divided into two categories with different energies, which present two characteristic peaks in the vibrational spectrum of atmospheric pressure ices.[20,21] Our previous simulations on ice XVI, XVII, and sI showed that the behavior of HBs of clathrate ice is very similar to ordinary ice, such as ice Ih.[22−24]

Due to the mixing of guest molecules, it is difficult to analyze the vibrational spectrum, especially in the far-IR region. In this study, the HB vibrations of sH and sII gas hydrates were investigated using density functional theory (DFT). We simulated IR, Raman, and phonon density of states (PDOS) spectra and examined the characteristic vibration modes. The PDOS curve reproduced the two HB peaks of the INS spectrum. The lattice dynamics analysis showed that the rule of two kinds of HB vibration modes still holds.

COMPUTING METHODS

The clathrate ice structure is a network of HBs supported by guest molecules (especially in sH). Methane can be trapped in the sI, sII, and sH types of clathrate hydrates. We focused on sII and sH gas hydrates with common guests. In sII, one unit cell contains 136 water molecules. We selected eight propane molecules filled in 5^{12} cages, with $5^{12}6^4$ cages accommodating 16 methane molecules. sH contains 34 water molecules per cell, including two neohexane molecules in the $5^{12}6^8$ cavities and six and four methane molecules in the $4^35^66^3$ and 5^{12} cavities, respectively. The crystallographic structure of sII propane−methane hydrate has been reported by Udachin et al.[25] The equilibrium data and structural characteristics of sH neohexane−methane hydrate have been reported by Seo et al.[26,27]

We constructed sII and sH type crystal structures using GenIce software, which rearranged the hydrogen atoms randomly in accordance with the Bernal−Fowler rules.[28,29] The zero-total-dipole-moment structure was chosen. The two structures are presented as S1 and S2, respectively, in the Supporting Information files.

The CASTEP code, a first-principles DFT package, was employed for this study.[30] According to our previous tests, we chose the revised Perdew−Burke−Ernzerhoff (RPBE) exchange−correlation (XC) functional of the general gradient approximation (GGA).[31] Although the RPBE functional slightly underestimates the intermolecular HBs, it is the best choice for vibrational spectrum simulation of ice crystals.[21] The norm-conserving pseudopotential was used to perform phonon calculations with a linear response method. To eliminate virtual frequencies, the geometry optimization convergence criterion for the energy and self-consistent field (SCF) were both set up to 1.0×10^{-9} eV/atom. The plane wave energy cutoff was 750 eV, and the K−point mesh was set at the γ point due to a big supercell. The hydrostatic pressure was 1 MPa. Thus, the propane−methane sII and neohexane−methane sH were stable under ambient conditions.[32,33] For property calculations, we selected "Phonons" including LO−TO splitting and "Polarization and IR and Raman spectra" including Raman intensities. We thus simulated PDOS, IR, and Raman curves of the two structures. Unfortunately, the calculation of the Raman spectrum on sII failed, maybe due to such a big supercell.

RESULTS AND DISCUSSION

Figure 1 presents the calculated PDOS curves in the range below 1100 cm^{-1} compared with the INS experimental

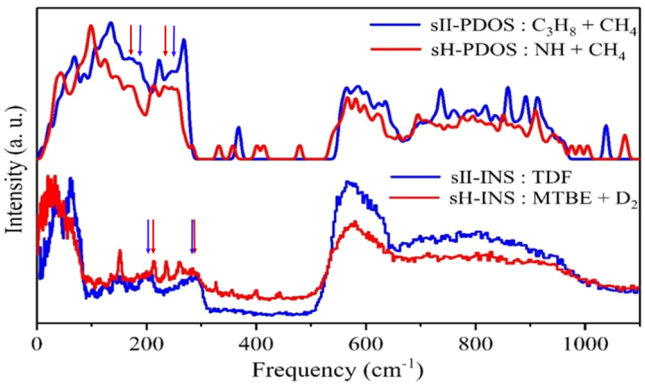

Figure 1. Comparisons of two INS data and two simulated PDOS curves of sII (blue line) and sH (red line) gas hydrates. Note that the guest molecule of sII-INS is tetrahydrofuran (TDF) and those of sH-INS are methyl *tert*-butyl ether (MTBE) and deuterium (D_2). The calculated model of sII contains propane (C_3H_8) and methane (CH_4), whereas that of sH contains neohexane (NH) and methane (CH_4). The two HB peaks of each model are marked with arrows.

spectra;[15] this represents the translation and libration region of clathrate ice. We constructed sI and sH structures with common guest molecules. However, the available INS experimental data are not the same as shown in Figure 1. We compared these two experimental and two simulated curves together to show that the guests do not influence the positions of HBs. The INS spectrum of sII showed two distinct peaks at 208 and 292 cm^{-1}, representing the two typical HB peaks of ice. Due to the contributions of methyl *tert*-butyl ether in sH, three extra peaks at 213, 235, and 260 cm^{-1} were superpositioned on the HB peaks. The PDOS curves of sII and sH clearly showed a strong HB band at above 200 cm^{-1}, with some sharp peaks overlapped by guest molecules. The weak HB peaks were visible as a hump below 200 cm^{-1}, superpositioned with acoustic phonons. Since the INS experiments collected signals throughout the whole Brillouin zone, including dispersion effects, and the RPBE functional underestimates the intermolecular interactions, the calculated peaks show a red shift compared with the experiments. The vibration frequency is very sensitive to bond length. The calculated average HB length of sII was 1.916 Å; this was a bit shorter than that of sH (1.925 Å). Thus, the HB peaks of sII showed a blue shift compared with those of sH. The trend is consistent with the experimental INS spectra. The influences of the guest molecules are discussed in detail later in the text.

The two HB peaks of ice were first identified in an INS experiment by Li et al.[34] Li then proposed the existence of two HB force constants that resulted in the energy splitting of HB peaks.[35] This sparked a debate on the mechanism underlying HBs.[36−38] Bertie et al. suggested that the strength of the HBs in hydrates was very similar to those in ice.[39] Based on simulations of ice phases, we found that the HB vibration modes in an ice crystal lattice could be classified into two: the two-bond mode and the four-bond mode.[20,21] And this rule also applies to clathrate ice.[22−24]

https://doi.org/10.1021/acsomega.3c01237
ACS Omega 2023, 8, 11634−11639

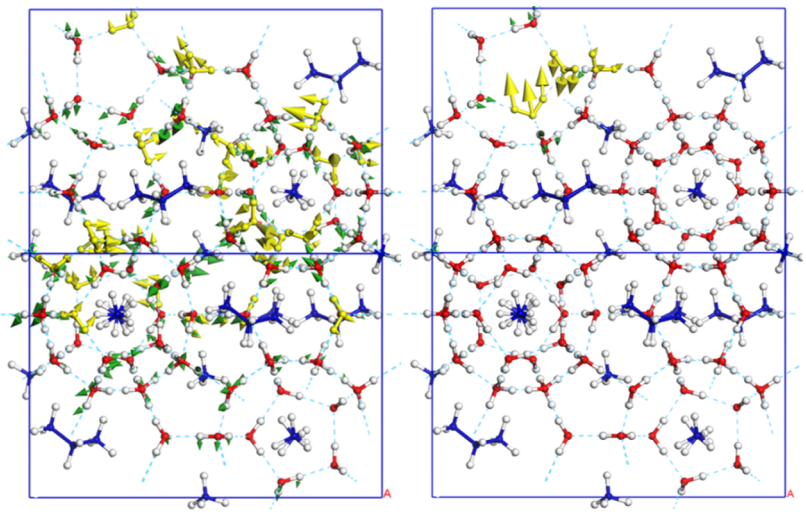

Figure 2. Examples of two HB vibration modes of sII gas hydrates. (a) Two-bond mode at 196 cm^{-1}. (b) Four-bond mode at 277 cm^{-1}. The oxygen and carbon atoms are colored red and blue. Typical vibration modes are colored gold.

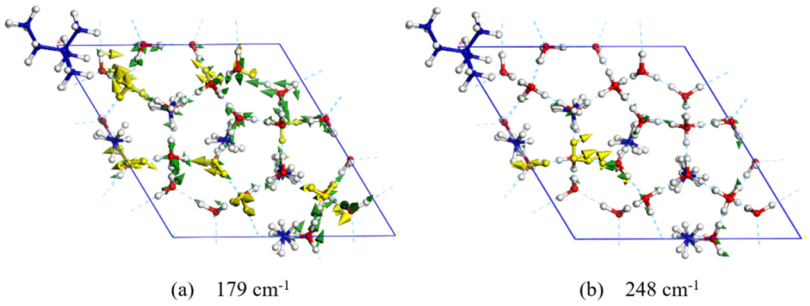

Figure 3. Examples of two HB vibration modes of sH gas hydrates. (a) Two-bond mode at 179 cm^{-1}. (b) Four-bond mode at 248 cm^{-1}. The green arrow represents the vibration direction, with size being proportional to amplitude.

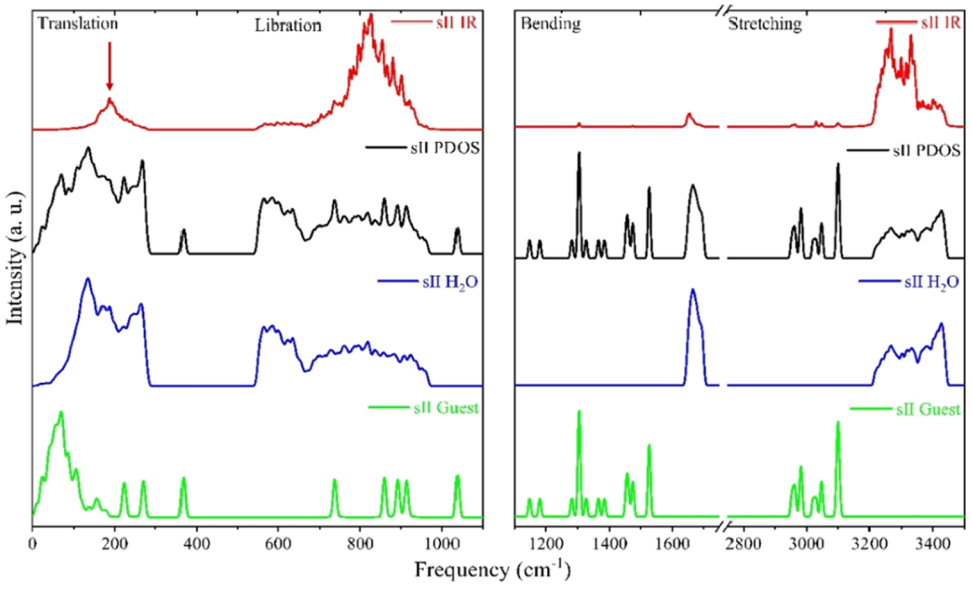

Figure 4. Simulated spectra of sII gas hydrates in the 0−1100 cm^{-1} region (left) and 1150−3500 cm^{-1} region (right). The four curves from top to bottom correspond to IR, PDOS, and partial PDOS of ice crystals and guest molecules. The red arrow indicates the weak HB peak of SII in the IR spectrum.

Figures 2 and 3 show examples of two HB vibration modes in sII and sH. One water molecule in an ice lattice links four neighbors via HBs. Due to the restrictions of the local tetrahedral structure, the center molecule may vibrate along

https://doi.org/10.1021/acsomega.3c01237
ACS Omega 2023, 8, 11634−11639

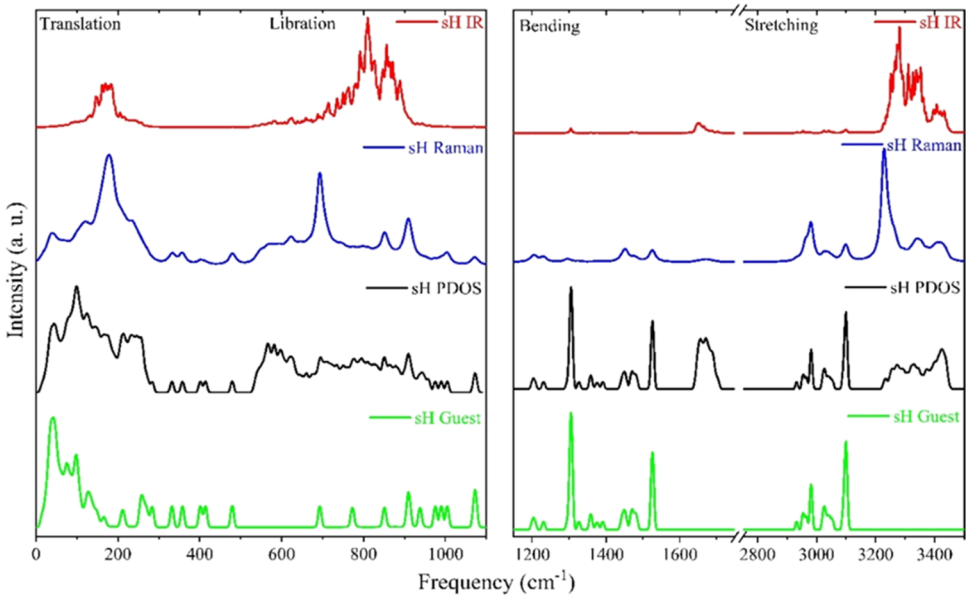

Figure 5. Simulated spectra of sH gas hydrates in the 0−1100 cm^{-1} region (left) and 1150−3500 cm^{-1} region (right). The four curves from top to bottom correspond to the IR, Raman, PDOS, and partial PDOS of guest molecules. The IR and Raman spectra can only reflect the two-bond modes due to selection rules.

Table 1. Comparisons of Simulated HB Peaks (cm^{-1}) with Those in the Literature

		PDOS	INS	IR/Raman (this work)	simulations (literature)	experiments
weak HB	sII	196	208[a]	187	184[b]	218[c]/222[d]/235[e]
	sH	179	213[a]	169/179	186[f]	
strong HB	sII	277	292[a]			
	sH	248	293[a]			

[a]Ref 15. [b]Ref 17. [c]Ref 40. [d]Ref 41. [e]Ref 42. [f]Ref 19.

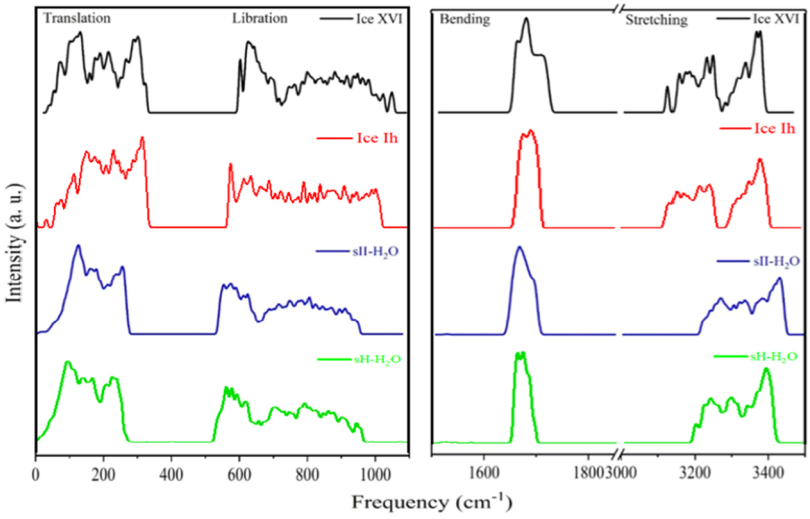

Figure 6. Comparisons between clathrate ice sII, ice SH, ice Ih, and ice XVI. The partial PDOS of guest molecules has been properly subtracted.

the angular bisector of H−O−H. Thus, the four HBs work together against their four neighbors. This represents the four-bond mode, which is strong. Alternatively, it can vibrate along two HBs while keeping the other two unchanged. This represents the two-bond mode, which is weak. For the dynamic process examples, please see the Supporting files, which are in S3 and S4.

Figures 4 and 5 show the simulated vibrational spectra of sII and sH. To compare with the values in the literature, the two HB peaks are listed in Table 1. One can see that the simulated peaks show a slight red shift. The two peaks of sII are located at 196 and 277 cm^{-1}, while the two peaks of sH are located at 179 and 248 cm^{-1}.

Neither IR nor Raman measurements could distinguish the strong HB peak, and neutron scattering may detect all the water-related phonons due to the presence of different interaction mechanisms. To determine the effects of guest molecules, the total and partial PDOS of ice and guest

https://doi.org/10.1021/acsomega.3c01237
ACS Omega 2023, 8, 11634−11639

molecules were derived, as shown in Figure 4. As the HBs are saturated along the clathrate ice lattice, there were no HB interactions between the water and guest molecules. That is, the vibration modes of the HB and guest molecules were separate. Figure 4 shows three main peaks below 300 cm^{-1} of clathrate ice: acoustic phonons, weak HB, and strong HB. This was very similar to ice Ih.[21] Due to the larger bond length than ice Ih, the HB peaks in sII showed a red shift compared with ice Ih. The libration region of ice, representing the water rotation modes, was 500 to 1000 cm^{-1}. The region of intramolecular H−O−H bending was around 1700 cm^{-1} and that of O−H stretching was above 3200 cm^{-1}. The contributions of guest molecules can be seen clearly in these two figures.

Ice XVI is an sII-type clathrate structure. Details of the vibration modes and simulated spectra can be found in our previous study.[22] We compared the PDOS curves of these four structures, as shown in Figure 6. In the translation region, the HB peaks of sII or sH show a clear red shift compared with ice XVI (bond length 1.827 Å). In the intramolecular OH stretching region, the vibration bands of sII and sH show a clear blue shift. On account of the longer bond length than ice Ih, the HB peaks in clathrate ice should present a red shift, while the intramolecular OH strength shows a blue shift compared with ice Ih. Due to hydrogen disorder, the vibration modes were nondegenerate. Thus, many adjacent vibration modes are coupled to form a vibration band. However, as the ratio of vibrational frequencies was about $\sqrt{2}$ between the two HB vibration modes,[21] the gap between the two HB peaks was obvious. Overall, the four spectra were quite similar.

We next discuss the contributions of guest molecules. As can be seen in the left panel of Figure 4, the IR absorption peak at about 187 cm^{-1} shows the weak HB absorption band of clathrate ice. There were three sharp peaks of PDOS from neohexane at 224, 271, and 368 cm^{-1}, respectively. However, they are not IR active. It is the same behavior as that of sH in Figure 5. Although there were multiple peaks from guest molecules, they contributed very little to the IR and Raman spectra in the far-IR region.

To date, energy recovery from gas hydrates has not been commercialized due to economy and safety concerns. In terms of physics, the dissociation of gas hydrates is mediated by HB fracture. Thus, supplying energy directly to HBs would be an efficient way of dissociating gas hydrates. As the IR absorption of gas hydrates showed only a HB peak in this region, it was likely difficult for the guest molecules to absorb IR energy. An INS experiment on liquid water showed a valley in the range of the two HBs;[43] this was probably because the water molecules in liquid water do not form a stable tetrahedral structure. If one were to provide a terahertz laser (at about 6 THz) supply to gas hydrates, the resonance absorption may decompose the clathrate ice and release the guest molecules with minimum energy loss. Nowadays, the experiment of high-power terahertz laser above 4 THz is still difficult to achieve. We plan to perform this kind of photon−phonon resonance absorption experiment in the near future.

CONCLUSIONS

We used a first-principles DFT method to investigate the vibration spectra of sII and sH gas hydrates. Applying the principle of two HB vibration modes, we focused on the translation band of clathrate ice. We found that there was almost no coupling between the water and guest molecules. After subtracting the components of guest molecules, the vibration spectra of sII and sH gas hydrates became very similar to that of clathrate ice. Importantly, the IR absorption in this region was from HBs. Since liquid water does not exhibit strong absorption in this region compared to gas hydrates, we propose a new method to exploit gas hydrates using a high-power terahertz laser at about 6 THz. The resulting resonance absorptions of HBs may lead to the rapid melting of clathrate ice and release of natural gas with minimum energy loss. The development of such a THz laser may foster novel experiments on rapid ice melting.

ASSOCIATED CONTENT

Supporting Information

The Supporting Information is available free of charge at https://pubs.acs.org/doi/10.1021/acsomega.3c01237.

Structure of SII (S1) (CIF)

Structure of SH (S2) (CIF)

Dynamic analysis of SH's two-bond vibration at 179 cm^{-1} (S3) (MP4)

Dynamic analysis of SH's four-bond vibration at 248 cm^{-1} (S4) (MP4)

AUTHOR INFORMATION

Corresponding Author

Peng Zhang − *School of Space Science and Physics, Shandong University, Weihai 264209, China;* orcid.org/0000-0002-1099-6310; Email: zhangpeng@sdu.edu.cn

Authors

Qing Guo − *School of Space Science and Physics, Shandong University, Weihai 264209, China*

Hao-Cheng Wang − *Tsinghua Shenzhen International Graduate School, Tsinghua University, Shenzhen 518055, China*

Xiao-Yan Liu − *School of Space Science and Physics, Shandong University, Weihai 264209, China*

Xiao-Qing Yuan − *School of Space Science and Physics, Shandong University, Weihai 264209, China*

Xiao-Tong Dong − *School of Space Science and Physics, Shandong University, Weihai 264209, China*

Yi-Ning Li − *School of Space Science and Physics, Shandong University, Weihai 264209, China*

Yi Yin − *School of Space Science and Physics, Shandong University, Weihai 264209, China*

Complete contact information is available at: https://pubs.acs.org/10.1021/acsomega.3c01237

Notes

The authors declare no competing financial interest.

ACKNOWLEDGMENTS

We are grateful for financial support provided throughout the project ZR2022MA017 supported by Shandong Provincial Natural Science. The numerical calculations were performed on the supercomputing system at the Supercomputing Center, Shandong University, Weihai.

REFERENCES

(1) Sloan, E. D. Fundamental principles and applications of natural gas hydrates. *Nature* **2003**, *426*, 353−359.

(2) Claussen, W. F. A second water structure for inert gas hydrates. *J. Chem. Phys.* **1951**, *19*, 1425−1426.
(3) Ripmeester, J. A.; Ratcliffe, C. Xenon-129 NMR studies of clathrate hydrates: new guests for structure II and structure H. *J. Phys. Chem. A* **1990**, *94*, 8773−8776.
(4) Ripmeester, J. A.; Tse, J. S.; Ratcliffe, C. I.; Powell, B. M. A new clathrate hydrate structure. *Nature* **1987**, *325*, 135−136.
(5) Kim, E.; Seo, Y. A novel discovery of a gaseous sH clathrate hydrate former. *Chem. Eng. J.* **2019**, *359*, 775−778.
(6) Falenty, A.; Hansen, T. C.; Kuhs, W. F. Formation and properties of ice XVI obtained by emptying a type sII clathrate hydrate. *Nature* **2014**, *516*, 231−233.
(7) del Rosso, L.; Celli, M.; Ulivi, L. New porous water ice metastable at atmospheric pressure obtained by emptying a hydrogen-filled ice. *Nat. Commun.* **2016**, *7*, No. 13994.
(8) Schicks, J. M.; Ripmeester, J. A. The coexistence of two different methane hydrate phases under moderate pressure and temperature conditions: Kinetic versus thermodynamic products. *Angew. Chem., Int. Ed.* **2004**, *43*, 3310−3313.
(9) Murshed, M. M.; Kuhs, W. F. Kinetic studies of methane−ethane mixed gas hydrates by neutron diffraction and Raman spectroscopy. *J. Phys. Chem. B* **2009**, *113*, 5172−5180.
(10) Sum, A. K.; Burruss, R. C.; Sloan, E. D. Measurement of clathrate hydrates via Raman spectroscopy. *J. Phys. Chem. B* **1997**, *101*, 7371−7377.
(11) Jin, Y.; Oyama, H.; Nagao, J. Infrared Spectroscopy of Gas Hydrate Dissociation Behavior During Depressurization. *Jpn. J. Appl. Phys.* **2009**, *48*, No. 108001.
(12) Gutt, C.; Baumert, J.; Press, W.; Tse, J. S.; Janssen, S. The vibrational properties of xenon hydrate: An inelastic incoherent neutron scattering study. *J. Chem. Phys.* **2002**, *116*, 3795−3799.
(13) Tse, J. S.; Powell, B. M.; Sears, V. F.; Handa, Y. P. The lattice dynamics of clathrate hydrates. An incoherent inelastic neutron scattering study. *Chem. Phys. Lett.* **1993**, *215*, 383−388.
(14) Tse, J. S.; Ratcliffe, C. I.; Powell, B. M.; Sears, V. F.; Handa, Y. P. Rotational and translational motions of trapped methane. Incoherent inelastic neutron scattering of methane hydrate. *J. Phys. Chem. A* **1997**, *101*, 4491−4495.
(15) Celli, M.; Colognesi, D.; Ulivi, L.; Zoppi, M.; Ramirez-Cuesta, A. J. Phonon density of states in different clathrate hydrates measured by inelastic neutron scattering. *J. Phys.: Conf. Ser.* **2012**, *340*, No. 012051.
(16) Tse, J. S.; Klein, M. L.; Mcdonald, I. R. Molecular dynamics studies of ice Ic and the structure I clathrate hydrate of methane. *J. Phys. Chem. B* **1983**, *87*, 4198−4203.
(17) Vlasic, T. M.; Servio, P. D.; Rey, A. D. Infrared Spectra of Gas Hydrates from First-Principles. *J. Phys. Chem. B* **2019**, *123*, 936−947.
(18) Ramya, K. R.; Kumar, G. V. P.; Venkatnathan, A. A Raman spectra of vibrational and librational modes in methane clathrate hydrates using density functional theory. *J. Chem. Phys.* **2012**, *136*, No. 174305.
(19) Daghash, S. M.; Servio, P.; Rey, A. D. From Infrared Spectra to Macroscopic Mechanical Properties of sH Gas Hydrates through Atomistic Calculations. *Molecules* **2020**, *25*, No. 5568.
(20) Zhu, X. L.; Cao, J. W.; Qin, X. L.; Jiang, L.; Gu, Y.; Wang, H. C.; Liu, Y.; Kolesnikov, A. I.; Zhang, P. Origin of Two Distinct Peaks of Ice in the THz Region and Its Application for Natural Gas Hydrate Dissociation. *J. Phys. Chem. C* **2020**, *124*, 1165−1170.
(21) Qin, X. L.; Zhu, X. L.; Cao, J. W.; Wang, H. C.; Zhang, P. Investigation of hydrogen bond vibrations of ice. *Acta Phys. Sin.* **2021**, *70*, No. 146301.
(22) Wang, Z. R.; Zhu, X. L.; Jiang, L.; Zhang, K.; Luo, H. W.; Gu, Y.; Zhang, P. Investigations of the Hydrogen Bonds and Vibrational Spectra of Clathrate Ice XVI. *Materials* **2019**, *12*, No. 246.
(23) Zhu, X. L.; Yuan, Z. Y.; Jiang, L.; Zhang, K.; Wang, Z. R.; Luo, H. W.; Gu, Y.; Cao, J. W.; Qin, X. L.; Zhang, P. Computational analysis of vibrational spectrum and hydrogen bonds of ice XVII. *New J. Phys.* **2019**, *21*, No. 043054.
(24) Wang, H. C.; Zhu, X. L.; Cao, J. W.; Qin, X. L.; Yang, Y. C.; Niu, T. X.; Lu, Y. B.; Zhang, P. Density functional theory studies of hydrogen bonding vibrations in sI gas hydrates. *New J. Phys.* **2020**, *22*, No. 093066.
(25) Udachin, K. A.; Lu, H.; Enright, G. D.; Ratcliffe, C. I.; Ripmeester, J. A.; Chapman, N. R.; Riedel, M.; Spence, G. Single crystals of naturally occurring gas hydrates: The structures of methane and mixed hydrocarbon hydrates. *Angew. Chem., Int. Ed.* **2007**, *46*, 8220−8222.
(26) Seo, Y.; Kang, S.-P.; Lee, J.; Seol, J.; Lee, H. Hydrate equilibrium data of the CH4+ C3H8 gas mixture and simulated natural gas in the presence of 2, 2-Dimethylbutane and methylcyclohexane. *J. Chem. Eng. Data* **2011**, *56*, 2316−2321.
(27) Seo, Y.; Kang, S.-P.; Jang, W.; Kim, S. Inhibition of natural gas hydrates in the presence of liquid hydrocarbons forming structure H. *J. Phys. Chem. B* **2010**, *114*, 6084−6088.
(28) Bernal, J. D.; Fowler, R. H. A theory of water and ionic solution, with particular reference to hydrogen and hydroxylions. *J. Chem. Phys.* **1933**, *1*, 515−548.
(29) Matsumoto, M.; Yagasaki, T.; Tanaka, H. GenIce: Hydrogen-Disordered Ice Generator. *J. Comput. Chem.* **2018**, *39*, 61−64.
(30) Clark, S. J.; Segall, M. D.; Pickard, C. J.; Hasnip, P. J.; Probert, M. I. J.; Refson, K.; Payne, M. C. First principles methods using CASTEP. *Z. Kristallogr. - Cryst. Mater.* **2005**, *220*, 567−570.
(31) Hammer, B.; Hansen, L. B.; Nørskov, J. K. Improved adsorption energetics within density-functional theory using revised Perdew-Burke-Ernzerhof functionals. *Phys. Rev. B* **1999**, *59*, 7413−7421.
(32) Abbondondola, J. A.; Fleischer, E. B.; Janda, K. C. Propane clathrate hydrate formation accelerated by xenon. *J. Phys. Chem. C* **2009**, *113*, 4717−4720.
(33) Mohammadi, A. H.; Richon, D. Equilibrium data of neohexane + hydrogen sulfide and neohexane+ methane clathrate hydrates. *J. Chem. Eng. Data* **2011**, *56*, 5094−5097.
(34) Li, J. C.; Ross, D. K.; Howe, L.; Hall, P. G.; Tomkinson, J. Inelastic incoherent neutron scattering spectra of single crystalline and polycrystalline ICE Ih. *Phys. B* **1989**, *156-157*, 376−379.
(35) Li, J.; Ross, D. K. Evidence for two kinds of hydrogen bond in ice. *Nature* **1993**, *365*, 327−329.
(36) Tse, J. S.; Klug, D. D. Comments on "Further evidence for the existence of two kinds of H-bonds in ice Ih" by Li et al. *Phys. Lett. A* **1995**, *198*, 464−466.
(37) Morrison, I.; Jenkins, S. First principles lattice dynamics studies of the vibrational spectra of ice. *Phys. B* **1999**, *263−264*, 442−444.
(38) Klotz, S.; Strässle, T.; Salzmann, C. G.; Philippe, J.; Parker, S. F. Incoherent inelastic neutron scattering measurements on ice VII: Are there two kinds of hydrogen bonds in ice. *Europhys. Lett.* **2005**, *72*, 576−582.
(39) Bertie, J. E.; Bates, F. E.; Hendricksen, D. K. The Far Infrared Spectra and X-Ray Powder Diffraction Patterns of the Structure I Hydrates of Cyclopropane and Ethylene Oxide at 100 K. *Can. J. Chem.* **1975**, *53*, 71−75.
(40) Schicks, J. M.; Erzinger, J.; Ziemann, M. A. Raman spectra of gas hydrates–differences and analogies to ice 1h and (gas saturated) water. *Spectrochim. Acta, Part A* **2005**, *61*, 2399−2403.
(41) Prasad, P. S. R.; Prasad, K. S.; Thakur, N. K. Laser Raman spectroscopy of THF clathrate hydrate in the temperature range 90−300 K. *Spectrochim. Acta, Part A* **2007**, *68*, 1096−1100.
(42) Tulk, C. A.; Klug, D. D.; Ripmeester, J. A. Raman spectroscopic studies of THF clathrate hydrate. *J. Phys. Chem. A* **1998**, *102*, 8734−8739.
(43) Wang, Y.; Dong, S. Neutron scattering studies of low-fraction H 2 O in silica gel. *Phys. Rev. B* **2003**, *68*, No. 172201.

https://doi.org/10.1021/acsomega.3c01237
ACS Omega 2023, 8, 11634−11639